N94-35965

WIND TUNNEL MEASUREMENTS ON A FULL-SCALE F/A-18 WITH A TANGENTIALLY BLOWING SLOT

WENDY R. LANSER

Ames Research Center
Moffett Field, California

Summary

A full-scale F/A-18 was tested in the 80- by 120-Foot Wind Tunnel at NASA Ames Research Center to measure the effectiveness of a tangentially blowing slot in generating significant yawing moments while minimizing coupling in the pitch and roll axes. Various slot configurations were tested to determine the optimum configuration. The test was conducted for angles of attack from 25° to 50°, angles of sideslip from −15° to +15°, and free-stream velocities from 67 ft/sec to 168 ft/sec. By altering the forebody vortex flow, yaw control was maintained for angles of attack up to 50°. Of particular interest was the result that blowing very close to the radome apex was not as effective as blowing slightly farther aft on the radome, that a 16-inch slot was most efficient, and that yawing moments were generated without inducing significant rolling or pitching moments.

Nomenclature

A_s	area of the slot = $w_s l_s$, ft^2
b	reference wing span, 37.42 ft
C_L	lift coefficient in body axes, lift/$q_\infty S$
C_m	body-axis pitching moment coefficient, pitching moment/$q_\infty Sc$
C_n	body-axis yawing moment coefficient, yawing moment/$q_\infty Sb$
C_p	pressure coefficient, $(p - p_\infty)/q_\infty$
C_{roll}	body-axis rolling moment coefficient,
C_Y	body-axis side force coefficient, side force/$q_\infty S$
c	reference mean aerodynamic chord, 11.52 ft
FS	fuselage station, inches (radome apex at FS 60.5)
h_s	height of blowing slot = 0.01 inches
l_s	slot length, inches
$\dot{m}_s$	mass flow rate of slot, $\rho_s V_s A_s$
$\dot{m}_{ref}$	reference mass flow rate, $\rho_\infty U_\infty S$, lbm/sec
MFR	mass flow ratio, $\dot{m}_s/\dot{m}_{ref}$
mdot	mass flow rate through the slot, lbm/sec^2
p	static pressure, lb/in.^{2}
p_∞	free-stream static pressure, lb/in.^{2}
q_∞	free-stream dynamic pressure, $1/2\rho_\infty U_\infty^2$, lb/ft^2
S	reference wing area, 400 ft^2
U	free-stream velocity, ft/sec
V_s	velocity at the slot exit, ft/sec
x	distance from nose apex along longitudinal axis
α	angle-of-attack, degrees
β	angle of side slip, degrees
Δ	change due to forebody flow control mechanism
δ_h	horizontal stabilator deflection, degrees
ρ_∞	free-stream air density, slugs/ft^3
ρ_s	air density at the slot exit, slugs/ft^3

Introduction

Current fighter aircraft configurations, designed for high-speed flight, consist of long slender forebodies that have experimentally been shown to encounter strong asymmetric flow separation on the forebody at high angles of attack. The airflow over the upper surfaces of the aircraft at these angles of attack is separated and largely unsteady while the rudder effectiveness of the aircraft decreases as the vertical tails become engulfed in the wake of the forebody and the wings. This separated flow introduces significant side forces on the forebody even when little or no sideslip is present: the induced side force results in large yawing moments.

Future fighter-aircraft configurations will be subject to maneuvers at these high angles of attack that include the post stall region. More specifically, maneuvers will include the ability to rapidly pitch the nose down so that high-speed, low-angle of attack flight can be resumed, and the ability to rapidly roll the aircraft about the velocity vector in order to achieve a tighter turn radius (ref. 1). At these angles, the roll about the velocity vector is accomplished by controls that generate yawing moments along the body axes of the aircraft preferably without producing rolling or pitching moments.

A great deal of research has used the asymmetric flow separation on the slender forebody of the aircraft in order to improve yaw control at these high angles of attack. A yaw control device on the forebody has a significant mechanical advantage over a yaw control device on the vertical tail because the distance from the forebody to the aircraft center of gravity (cg) is greater than the distance from the vertical tail to the cg, and thus provides a greater moment arm. Additionally, the forebody with yaw control is unaffected by unsteady separated flow from the fuselage and wings. Yaw control devices tried in the past include forebody strakes, forward and aft blowing on the forebody through jet nozzles, jet blowing in combination with forebody strakes, tangential slot blowing on the forebody, and forebody jet nozzle blowing with the nozzles canted both windward and leeward (refs. 2–13). All of these devices were tested on small-scale models in water tunnels or wind tunnels.

As part of the NASA High Alpha Technology Program at NASA Ames Research Center, a full-scale F/A-18 was tested in the 80- by 120-Foot Wind Tunnel of the National Full-Scale Aerodynamic Complex (ref. 14). In these tests, several different methods of forebody flow control were examined to improve the lateral-directional control of the aircraft at high angles of attack. These methods included an aft-blowing circular-jet, a tangentially blowing slot, and deployable strakes. All of the techniques provided lateral control by manipulating the structure of the vortices shed from the forebody at high angles of attack. The effectiveness of these forebody flow control devices in generating lateral force and yawing moments are reported in references 9 and 10. This paper will present the effectiveness of various tangentially blowing slot configurations in generating yawing moment while minimizing the coupling between the aerodynamic forces and moments induced by the slot blowing.

Description of Model

The full-scale F/A-18A aircraft tested in the 80- by 120-Foot Wind Tunnel and shown in figure 1 is a single-seat aircraft built by the McDonnell Douglas Aircraft and Northrop corporations. The F/A-18A fighter aircraft has two vertical stabilizers canted 20° outboard from the vertical position and has leading edge extensions (LEXs) on each side of the fuselage just forward of the wing. The LEXs used for this experiment were the same instrumented ones that were flown on the High Alpha Research Vehicle at the Dryden Flight Research Facility in 1990 (ref. 15). During the wind tunnel test, the aircraft had both aircraft engines removed but air was free to flow through the inlets. The wingtip missile launch racks were mounted. The flaps were configured for high angle of attack flight with the leading-edge flaps at 33° down and the trailing-edge flaps at 0°. The horizontal tails were operated on a flight control schedule that was a function of the angle of attack to maintain trimmed flight conditions. The rudders were fixed at 0° for the majority of the test, however some data were also collected with both rudders positioned 30° trailing-edge left.

The radome designed for this experiment was built from a composite laminate of fiberglass/foam/fiberglass and fabricated from a mold formed of the production-aircraft radome. Figure 2 shows the slot and the discrete jet arrangement on this radome. Only the port slot and jet were active. Care was taken to assure symmetry; the starboard geometry was made identical by using a dummy slot and jet. The blowing slot had a total length of 48 inches and began 3 inches aft of the radome apex. The slots were positioned at 90° and 270° from the windward side (bottom) of the radome. The active slot was at the 270° position (port-side) and was designed to blow tangential to the surface toward the leeward side of the radome. The 48-inch slot was divided into 24 separately controlled segments with each segment measuring 2 inches long. The slot height was 0.10 inches. The aft blowing jet experiment will not be discussed in this paper, however more detailed information on this configuration can be found in reference 10. Air for the slot was supplied by 125 psi compressors. The air passed through a plenum located in the cockpit of the aircraft, which functioned as a settling chamber before traveling to the slot. The hardware from the plenum to each of the 2-inch slot segments was nearly identical in order to maintain a constant total pressure across the length of the slot. The mass flow rate of the blowing air was measured using a turbine flow meter.

A three-strut configuration was used to mount the F/A-18 aircraft in the 80-by 120-Foot Wind Tunnel test section on a rotatable balance frame. The aircraft was attached to a circular cross beam at the two main landing gear positions, which, in turn was attached to the wind-tunnel main struts. A tail boom assembly connected the aircraft at each engine mounting pin, and the arresting tail hook was used to attach the aircraft to the third wind-tunnel tail strut. The angle of attack was varied by changing the length of the tail strut while sideslip angle was changed by rotating the entire balance frame. This mounting arrangement placed the cross beam 33 feet above the test section floor, as shown in figure 1.

Description of Experiment

This experiment measured the effect of a tangentially blowing slot on the aircraft forces and moments. The results presented show the yawing moment generated by the slot blowing and the induced coupling between the aerodynamic forces and moments. To evaluate the effect of the tangential slot blowing, the differences in forces and moments were measured between the blowing-off and blowing-on conditions.

Test conditions included angle of attack variation from 25° to 50°, angles of sideslip from –15° to +15°, and freestream velocity from 67 ft/sec to 168 ft/sec. The Reynolds number based on wing mean aerodynamic chord ranged from 4.5×10^6 to 12.0×10^6. The mass flow rate of air blown through the slot configurations presented in this paper varied from 0 to 1.3 lb_m/sec. Force and moment data for different slot configurations, blowing rates, freestream velocities, Reynolds numbers, angle of attack, and angle of sideslip are presented. The test conditions match flight speeds and Reynolds number for 1 g flight, a fact of particular importance in forebody flow control experiments because the boundary layer in the forebody region developed and transitioned from laminar to turbulent as it would in flight.

The various slot configurations were studied to determine the optimum configuration, that is the configuration which produced the largest change in yawing moment for the minimum required blowing. The parameters that were varied in order to determine the optimum configuration were the slot length, the slot position relative to the radome apex, and the mass flow rate through the slot. The aircraft forces and moments used to evaluate the blown slot performance were measured using the wind-tunnel scale system and, are shown in the body axes coordinate system. The rudders were positioned at 0° deflection unless noted otherwise.

Results

Tangential Slot Blowing Optimization

The yawing moments generated by four different slots are shown in figure 3. The slots were 8, 16, 32, and 48 inches long and each began 3 inches from the radome apex. For each of the slot configurations, yawing moment increased as angle of attack increased. The mass flow ratio (MFR) through each of the slots varied with slot length. Comparing the results at these conditions, the 32-inch and the 48-inch long slots had the largest effect on the yawing moment throughout the entire angle-of-attack range.

The position of the slot relative to the radome apex also had an effect on the amount of side force generated by the device. The various slot positions relative to the radome apex are shown in figure 4. Figure 5(a) shows that for a MFR of 0.00026, the 16-inch slot positioned at 3 inches was not as effective as when positioned 11 or 19 inches aft of the radome apex. It is important to note that the 16-inch slot positioned at 11 or 19 inches produced nearly the same moments as the 32 or the 48-inch-long slots positioned at 3 inches (fig. 3) for a lower mass flow rate. This makes the 16-inch slot positioned 11 or 19 inches aft a more efficient configuration. Efficiency is important because if this concept was used in flight, the air supplied to the slot would come from the same source that supplies the pilot with the cockpit environment controls. This supply of air is limited. Figure 5(b), shows data for the same slot mass flow rate as in figure 5(a), however, the freestream velocity was increased yielding a lower MFR. For the lower MFR, the 16-inch slot positioned 11 and 19 inches aft of the radome apex again proved to be more effective than when positioned 3 inches aft of the radome apex. For comparison, the yawing moments produced by maximum rudder deflection are shown in figure 5(b). It is clear that slot blowing produced much larger moments than the maximum rudder deflection at these angles of attack.

The tangential slot blowing produced a side force in the direction of the blowing side of the radome. This result indicates that the tangential slot blowing keeps the flow attached along the blowing side of the radome. This flow phenomenon, called the coanda effect, creates a low-pressure on the blowing side of the radome resulting in a suction force. Thus, blowing from the left-side of the radome will produce a nose-left yawing moment. It was also noticed that blowing 11 or 19 inches aft of the apex allows this low pressure to affect more surface area, resulting in a greater yawing moment than for 3 inches aft of the apex. Additionally, the tighter radius very near the nose of the radome could defeat the coanda effect.

Based on the results presented above, the 16-inch and 32-inch slots beginning 11 inches aft of the radome apex were determined to be the most effective; consequently they were tested over an expanded range of mass flow rates. For a given yawing moment, the 16-inch slot used between 8% and 30% less mass flow than the 32-inch slot (fig. 6). Thus, the 16-inch slot is more efficient than the 32-inch slot. Both the 16- and 32-inch-long slots produced a small moment reversal at very low mass flow ratios. This moment reversal also appeared in the water tunnel experiments of slot blowing on the forebody of a fighter aircraft (ref. 5). This result may be related to results presented by Ericsson which showed side force reversals for a rotating circular cylinder at low rotation speeds (ref. 16).

In the 80- by 120-Foot Wind Tunnel experiments, the exit velocities through the slots ranged from subsonic flow to sonic flow as the mass flow through the slots was increased. The data in figure 6 includes exit velocities in both the subsonic and sonic regions. For the 40° angle-of-attack case, choked flow occurs at a mass-flow ratio of 0.00013 and 0.00023 for the 16- and 32-inch-long slots respectively. These data confirm that even when the exit velocity reached sonic conditions, the yawing moments continued to increase with increasing mass flow.

Tangential slot blowing proved to be effective across the entire angle-of-attack range. In fact, its effectiveness increased as the angle of attack was increased (fig. 7). Again the results indicate a small moment reversal at very low mass flow rates for the 40° and 50° angle of attack cases. Data were not taken for small mass flows at 30°.

The effect of Reynolds number was examined in the tunnel by testing various velocities up to the maximum of 168 ft/sec. Figure 8 shows the variation of yawing moment with MFR for the 16-inch slot 11 inches aft of the apex and at $\alpha = 40°$. Results are shown for various wind-tunnel velocities, and there is very little difference between the curves. These results indicate that slot blowing was not sensitive to Reynolds number across this range of velocities.

Aerodynamic Coupling

The results generated by the 16-inch slot positioned 11 inches aft of the radome apex are used to illustrate the coupling between the aerodynamic forces and moments induced by the slot blowing. The effects of angle of attack on pitching moment due to the slot blowing are shown in figure 9(a). As a point of reference, the pitching moment due to the horizontal tail deflection, which is the conventional pitch control mechanism, is also shown in figure 9(a). The changes in pitching moment for the two different blowing rates are nearly the same with the greatest change measured as 0.03 seen at 50° angle of attack. The pitching moment due to the horizontal tail deflection over the same angle-of-attack range shows that the moments generated by slot blowing are easily correctable. Similar results are seen in the lift-coefficient data (fig. 9(b)) which demonstrates that there is no significant lift generated by the blowing slot. The lift due to 30° of rudder deflection is shown on figure 9(b) as a reference point.

As shown previously, the slot blowing generates large side forces and yawing moments (figs. 10(a) and 10(b)). Furthermore, the magnitude of the side force and yawing moment is controlled by the blowing rate as seen from the two blowing conditions, 0.5 and 1.1 lb_m/sec. These forces and moments were produced while maintaining relatively small changes in rolling moments (fig. 10(c)), which is a desirable condition because roll-yaw coupling or pitch-yaw coupling complicates control implementation. The greatest changes in rolling moment, 0.011 and –0.006, were seen at the 35° and 50° angles of attack, respectively. Measurements taken on a 16% scale F-18 model with an aileron deflection of 25° down on the left and 25° up on the right, showed a ΔC_{roll} of 0.024 and 0.015 for angles of attack of 35° and 50°, respectively (ref. 6). Although model scaling effects have not been determined, these values indicate that the rolling moments produced by the blowing are correctable with control surface deflections and are only lightly coupled with the yawing and pitching moments.

The tangentially blowing slot showed similar results at sideslip angles ranging from –15° to +15° (fig. 11). The results for the side forces and yawing moments (figs. 11(a) and (b)), show that blowing on one side of the aircraft produces significant forces and moments when the aircraft is yawed in either direction. For example, if the aircraft had a natural tendency to yaw to the right ($-\beta$), blowing on the left-hand side of the radome would generate a nose left ($+\beta$) yawing moment. These data also show a well-behaved trend, though not linear, in the yawing moment produced for various blowing rates. The rolling moment generated by the blowing is again relatively small across the range of sideslip (fig. 11(c)), with the largest incremental change, 0.012, occurring at –10° sideslip.

Figures 12(a)–(c) show the change in lateral-directional characteristics due to the blowing. For these comparisons, data acquired with the F-18 production radome were used for the baseline no-blowing condition; no-blowing data are not available for the modified radome. The data in figure 12(a) show similar behavior to the data taken at 40° angle of attack (fig. 11(a)). Figure 12(b) shows that blowing has a larger effect on yawing moment as angle of attack was increased from $\alpha = 40°$ to $\alpha = 50°$. These results also show an increase in effectiveness as the blowing rate was increased. The effect of blowing on the rolling moment was small and nearly linear across the sideslip range tested (fig. 12(c)). The rolling moment induced by the blowing was better behaved at $\alpha = 50°$ than it was at $\alpha = 40°$. This result may indicate the roll-yaw coupling induced by the tangential blown slot decreases as angle of attack increases.

Conclusions

The primary objective of the research reported in this paper was to measure the effectiveness of a tangentially blowing slot in generating lateral-directional control of the F/A-18 at high angles of attack. It was shown that the tangential slot blowing produced significant yawing moments at high angles of attack. It was also found that blowing 11 inches aft of the radome apex was more effective than blowing 3 inches aft. The 16- and 32-inch-long slots were more effective and efficient than either the 8- or 48-inch-long slots. Additionally, the full-scale results showed that the effect of the tangential slot blowing on the yawing moment increased with the angle of attack, the angle of sideslip, and the mass flow of air blowing through the slot.

It was shown that the effects of the tangentially blowing slot were weakly coupled in pitch and roll. The magnitude of the induced forces and moments will be correctable with control surfaces.

References

1. Skow, A. M.: Agility as a Contributor to Design Balance. Journal of Aircraft, vol. 29, Nov. 1992, pp. 34–46.
2. Malcolm, G. N.: Forebody Vortex Control. AGARD-R-776, Paper No. 6, Mar. 1991.
3. Malcolm, G. N. and Ng, T. T.: Forebody Vortex Manipulation for Aerodynamic Control of Aircraft at High Angles of Attack. SAE Paper 892220, Sept. 1989.
4. Malcolm, G. N.; Ng, T. T.; Lewis, L. C.; and Murri, D. G.: Development of Non-Conventional Control Methods for High Angle of Attack Flight Using Vortex Manipulation. AIAA Paper 89-2192, Aug. 1989.
5. Ng, T., Suarez, C., and Malcolm, G.: Forebody Vortex Control Using Slot Blowing. AIAA Paper 91-3254, Sept. 1991.
6. Murri, D. G.; Biedeon, R. T.; Erickson, G. E.; Jordan, F. L.; and Hoffler, K. D.: Development of Actuated Forebody Strake Controls for the F-18 High Alpha Research Vehicle. NASA CP 3149, vol. 1, Nov. 1990, pp. 335–380.
7. LeMay, S. P.; Sewall, W.; and Henderson, J.: Forebody Vortex Flow Control on the F-16C Using Tangential Slot and Jet Nozzle Blowing. AIAA Paper 92-0019, Jan. 1992.
8. Gee, K.; Tavella, D.; and Schiff, L. B.: Computational Optimization of a Pneumatic Fuselage Forebody Flow Control Concept. AIAA Paper 91-3249, Sept. 1991.
9. Meyn, L. A.; Lar, W. R.; and James, K. D.: Full Scale High Angle of Attack Tests of an F/A-18: AIAA Paper 92-2676, June 1992.
10. Lanser, W. R.; and Meyn, L. A.: Forebody Flow Control on a Full-Scale F/A-18 Aircraft. AIAA Paper 92-2674, June 1992.
11. Gee, K.; Rizk, Y. M.; Murman, S. M.; Lanser, W. R.; Meyn, L. A.; and Schiff, L. B.: Analysis of a Pneumatic Forebody Flow Control Concept About a Full Aircraft Geometry. AIAA Paper 92-2678, June 1992.
12. Guyton, R. W.; and Maerki, G.: X-29 Forebody Jet Blowing. AIAA Paper 92-0017, Jan. 1992.
13. Krumenacker, J.; and Pellicano, P.: Flight Simulation and Data Analysis During a High Angle of Attack Vortex Flow Control Flight Test Program. AIAA Paper 92-4108, Aug. 1992.
14. Corsiglia, V. R.; Olson, L. E.; and Falarski, M. D.: Aerodynamic Characteristics of the 40- by 80/80- by 120-Foot Wind Tunnel at NASA Ames Research Center. NASA TM-85946, April 1984.
15. Fisher, D.; Banks, D.; and Richwine, D. M.: F-18 High Alpha Research Vehicle Surface Pressures: Initial In-Flight Results and Correlation With Flow Visualization and Wind-Tunnel Data. AIAA Paper 90-3018, Aug. 1990.
16. Ericsson, L. E.: Moving Wall Effects in Unsteady Flow. AIAA Paper 87-0241, Jan. 1987.

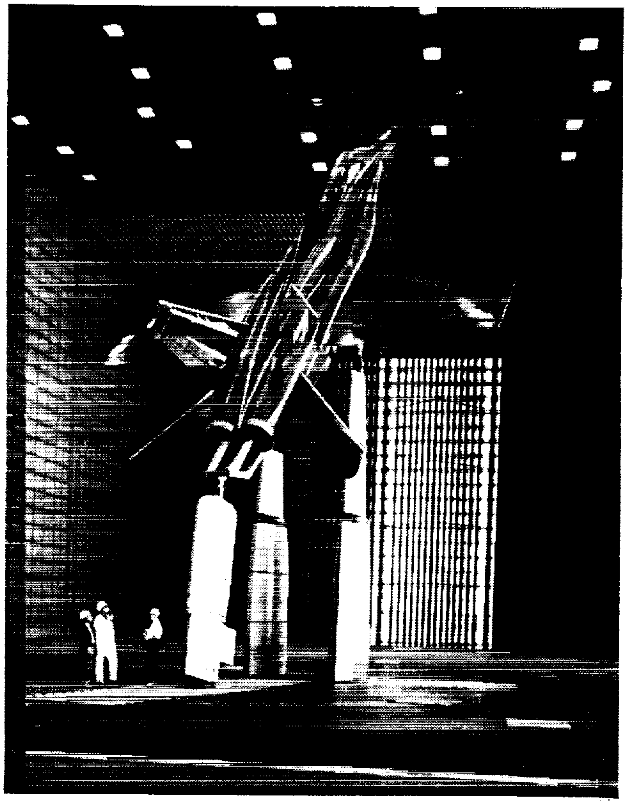

Fig. 1 Photograph of the F/A-18 mounted in the 80- by 120-Foot Wind Tunnel test section. A three-strut configuration with mounting hardware was used.

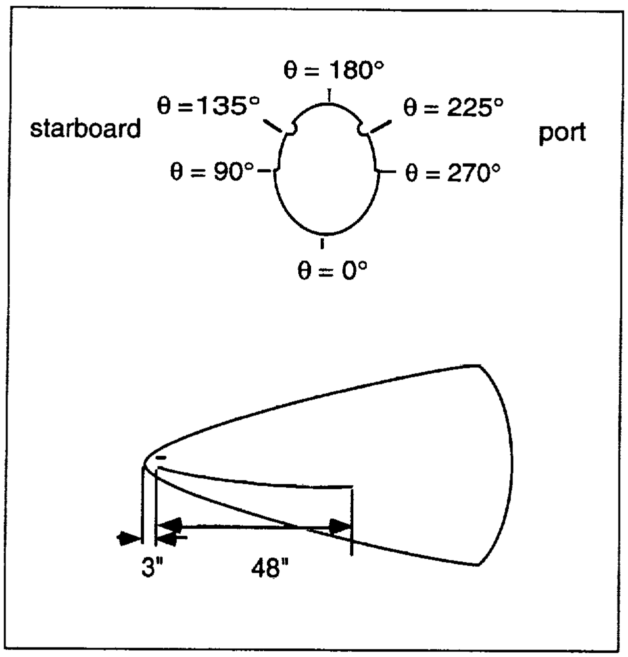

Fig. 2 The slot and discrete jet arrangement on the radome. The active slot and jet were located on the port side with the dummy slot and jet on the starboard side.

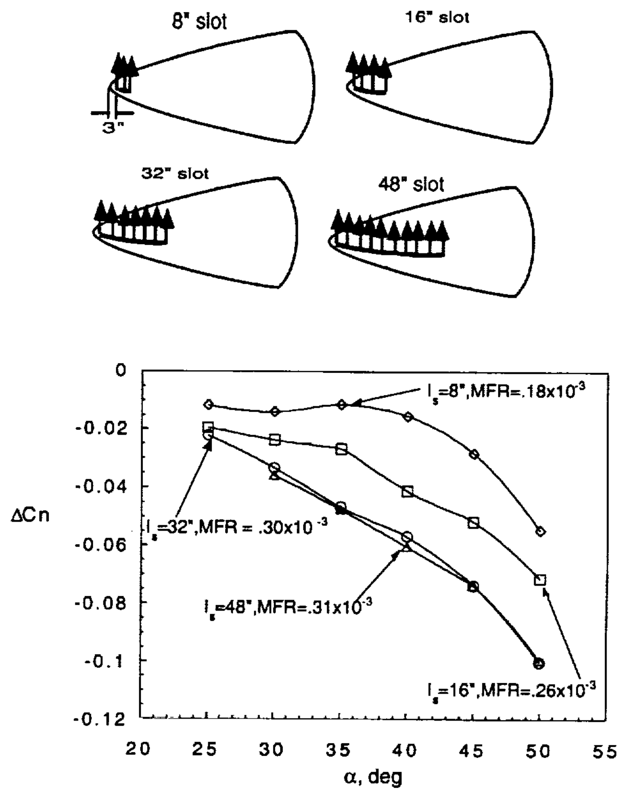

Fig. 3 The effect of angle of attack on yawing-moment coefficient in body axes for 4 different slot lengths; each slot began 3 inches aft of the radome apex: $\beta = 0°$, $U_\infty = 132$ ft/sec.

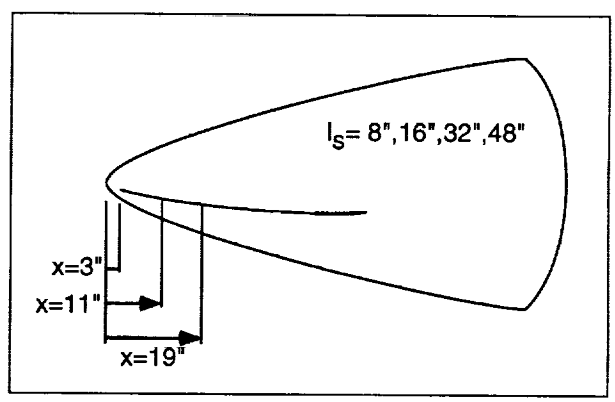

Fig. 4 Schematic of the various slot positions relative to the radome apex.

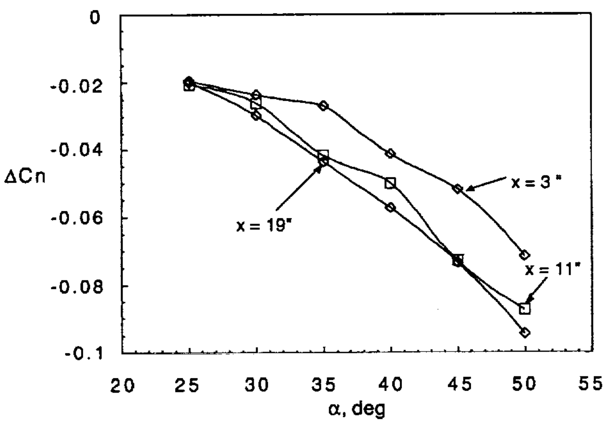

(a) U_∞ = 132 ft/sec, MFR = 0.26 x 10^{-3}

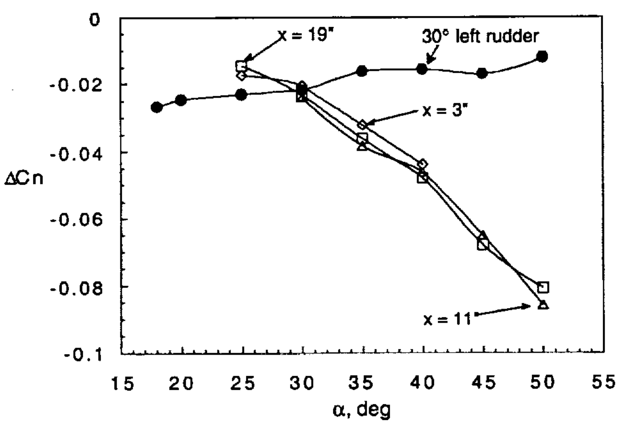

(b) U_∞=167 ft/sec, MFR = 0.22 x 10^{-3}

Fig. 5 Effect of angle of attack on yawing-moment coefficient in body axes for various U_∞ and slot positions on the radome: l_S = 16 inches, β = 0°.

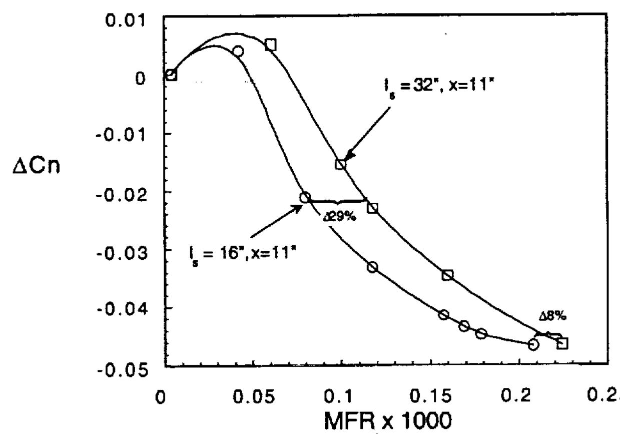

Fig. 6 Effect of the mass flow ratio on the yawing-moment coefficient in body axes: α = 40°, β = 0°, U_∞ = 168 ft/sec.

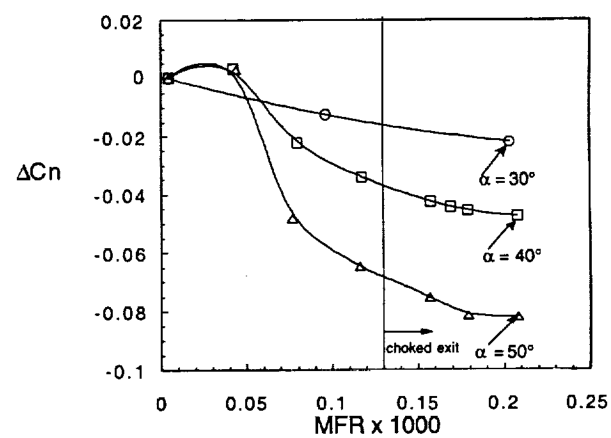

Fig. 7 Effect of mass flow ratio on yawing-moment coefficient in body axes for various angles of attack: l_S = 16 inches, β = 0°, U_∞ = 167 ft/sec.

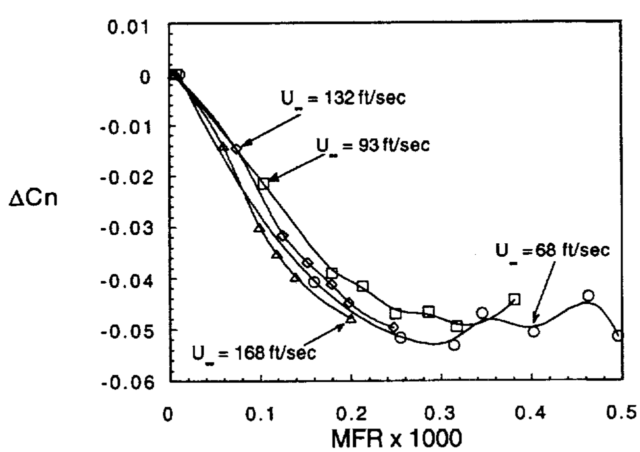

Fig. 8 Effect of mass flow ratio on the yawing-moment coefficient in body axes for various free-stream velocities: α = 40°, β = 0°, l_S = 16 inches, x = 11 inches.

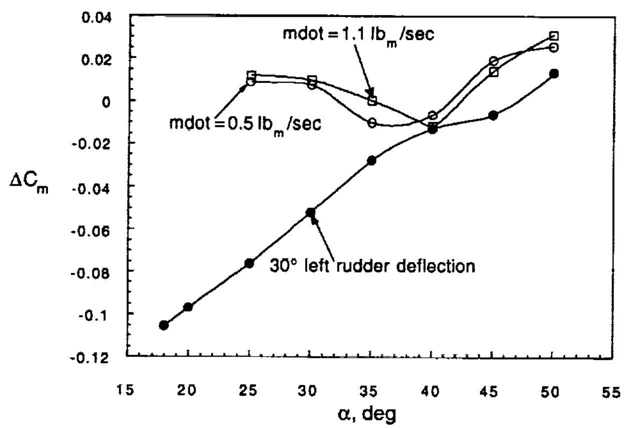

(a) Effect of angle of attack on pitching-moment coefficient in body axes.

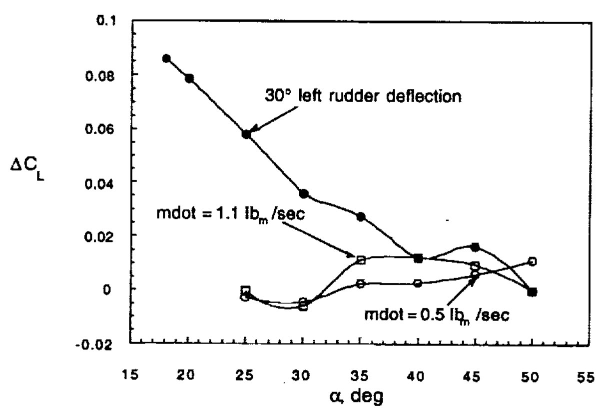

(b) Effect of angle of attack on lift coefficient in body axes.

Fig. 9 Effect of angle of attack on the longitudinal characteristics due to port-side slot blowing for two blowing rates: U_∞ = 168 ft/sec, $\beta = 0°$, $\delta_h = f(\alpha)$.

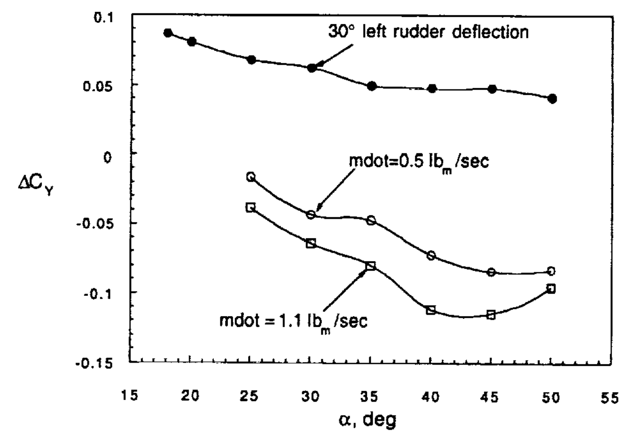

(a) The effect of angle of attack on side force coefficient in body axes.

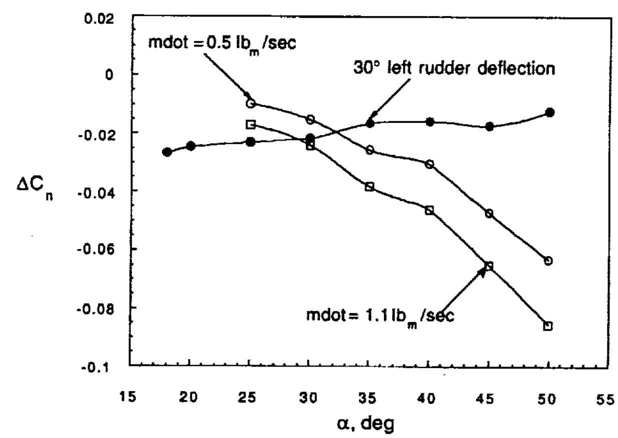

(b) Effect of angle of attack on yawing-moment coefficient in body axes.

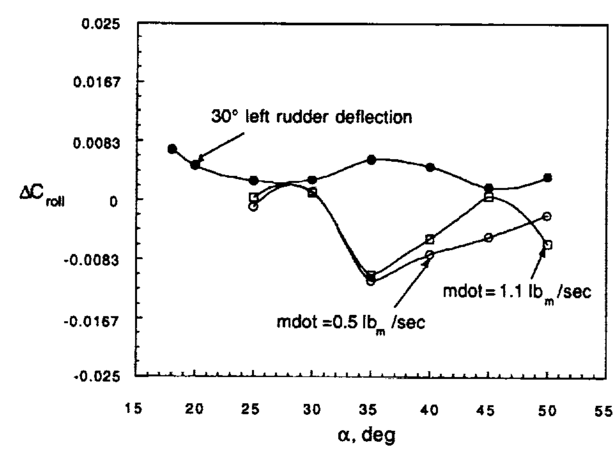

(c) Effect of angle of attack on rolling-moment coefficient in body axes.

Fig. 10 Effect of angle of attack on the lateral-directional characteristics due to port-side slot blowing for two blowing rates: U_∞ = 168 ft/sec, $\beta = 0°$, $\delta_h = f(\alpha)$.

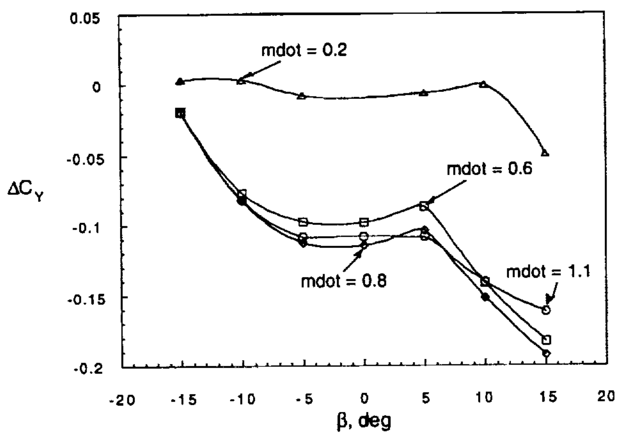

(a) Effect of sideslip angle on side-force coefficient in body axes.

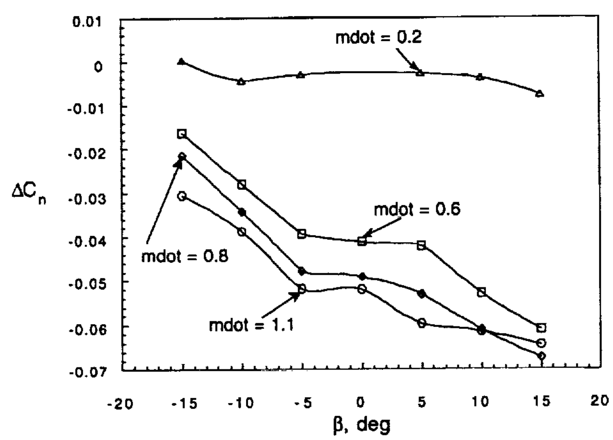

(b) Effect of sideslip angle on yawing-moment coefficient in body axes.

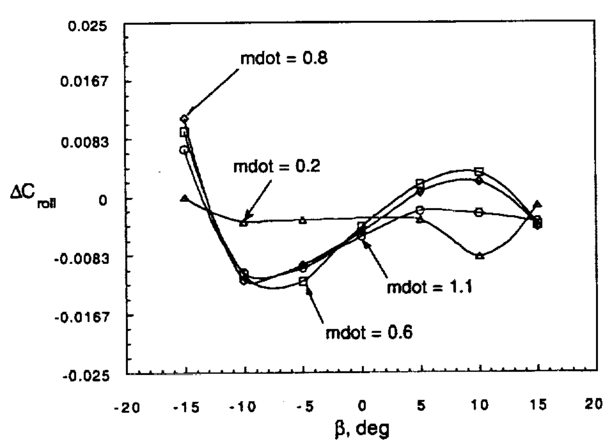

(c) Effect of sideslip angle on rolling-moment coefficient in body axes.

Fig. 11 Effect of sideslip angle on the lateral-directional characteristics due to port-side blowing for various blowing rates in lb_m/sec: $U_\infty = 132$ ft/sec, $\alpha = 40°$, $\delta_h = f(\alpha)$.

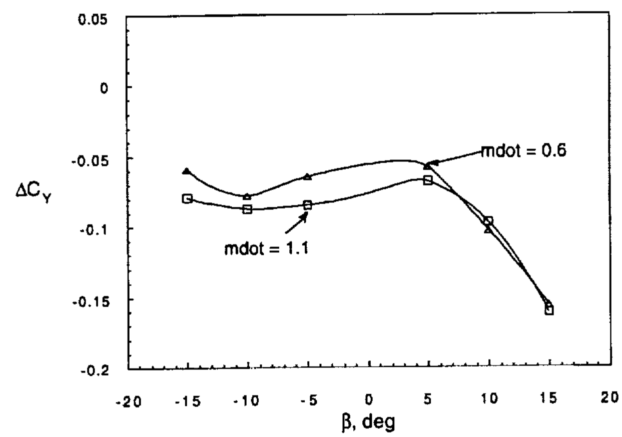

(a) Effect of sideslip angle on side-force coefficient in body axes.

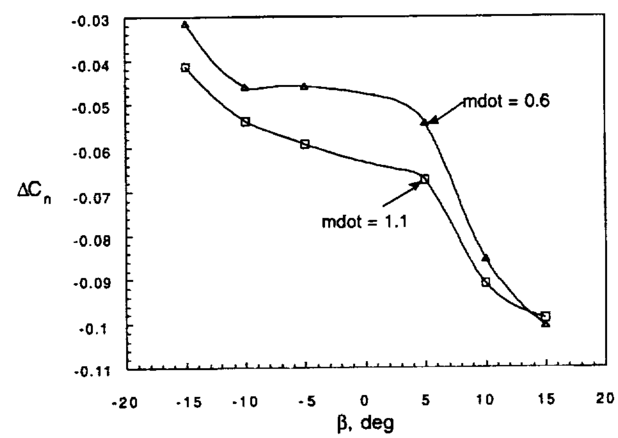

(b) Effect of sideslip angle on yawing-moment coefficient in body axes.

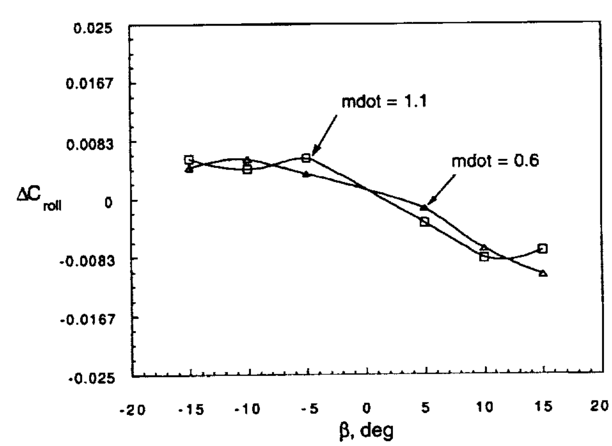

(c) Effect of sideslip angle on rolling-moment coefficient in body axes.

Fig. 12 Effect of sideslip angle on the lateral-directional characteristics when port-side blowing is active at several blowing rates in lb_m/sec: $U_\infty = 132$ ft/sec, $\alpha = 50°$, $\delta_h = f(\alpha)$.

Biography

Wendy Lanser began her career with NASA Ames as a co-op student at Dryden in 1985. As a co-op student she worked on the Oblique Wing and X-29 programs at Dryden and later at the Unitary Wind Tunnels. In 1988 she graduated from California Polytechnic State University in San Luis Obispo with a degree in Aeronautical Engineering. Upon graduation she began work in the Full-Scale Aerodynamics Division at Ames-Moffett. Currently she is working in the Fixed Wind Aerodynamics Branch, FFF, at the 80-by 120 Wind Tunnel. For the past three years Ms. Lanser has worked on the High Alpha Technology Program. Her role in the program has been a research engineer on the Full-Scale Wind Tunnel tests of an F-18 aircraft.

She also participates in the College Recruitment Program at Ames. Ms. Lanser can be reached at 604-3543 or M/S 247-2.